Analyst

Volume 1 | Number 1 | Jan 2013 | Pages 1–100

Analyst

www.rsc.org/analyst

ROYAL SOCIETY OF CHEMISTRY

ROYAL SOCIETY OF CHEMISTRY

www.rsc.org/analyst

Analyst

PAPER

On-chip monitoring of skeletal myoblast transplantation for the treatment of hypoxia-induced myocardial injury†

Juan He,[a]‡ Chao Ma,[b]‡ Wenming Liu[a] and Jinyi Wang[a,b]*

A comprehensive elucidation of unexpected adverse events occurred in skeletal myoblast transplantation is fundamental for the optimization of myocardial therapeutic effects. However, a well-defined method to study the interactions between skeletal myoblasts and cardiomyocytes during the healing process is out of reach. Here, we describe a microfluidic method for monitoring the interactions between skeletal myoblasts and hypoxia-injured cardiomyocytes in a spatiotemporally controlled manner, mimicking the in vivo cell transplantation process. A myocardial hypoxia environment was created using an oxygen consumption blocking reagent carbonyl cyanide 4-(trifluoromethoxy)phenylhydrazone. Meanwhile, the interactions between skeletal L6 myoblasts and hypoxia-injured myocardium H9c2 cells were investigated and the effects of L6 conditional medium on H9c2 cells were comparatively analyzed by quantitatively measuring the morphological and pathophysiological dynamics of H9c2 cells. The results showed that skeletal myoblasts could repair hypoxia-injured H9c2 cells mainly through direct cell-to-cell interactions. This simple on-chip assay for investigating myocardial repair processes may provide avenues for in vitro screening of drug-induced cardiotoxicity.

Introduction

Cardiovascular diseases, also called heart diseases, are the leading cause of morbidity and mortality, accounting for nearly one-third of deaths worldwide, and project to increase until at least 2030.[1] Heart transplantation remains the only definitive treatment for end-stage heart failure, but hindered by restricted availability of donor hearts and immunity rejection. Cell transplantation represents a novel approach for improving myocardial function,[2-4] as accumulating evidences from various experiments those have explored different cell types including embryonic stem cells,[5] cardiac myocytes,[6] fetal or neonatal cardiomyocytes,[7,8] skeletal myoblasts,[9,10] fibroblasts,[9] and hematopoietic stem cells.[2,11] Among them, skeletal muscle-derived myoblasts, because of their in vitro high proliferative potential, autologous availability without ethical issues and immune-suppression, highly resistance to ischemic stress, and a low risk of tumorgenicity,[12] remain the most well-studied donor cell types for myocardial repair and/or regeneration. However, differentiated skeletal myoblasts are distinguished with myocardial cells in electrophysiological characteristics, which can cause fatal ventricular arrhythmia in some patients early after cell transplantation.[13,14] Moreover, transplanted skeletal myoblasts may become an ectopic excitement site and new

born cells may produce a factor that can also induce/cause arrhythmia.[14] These emerged problems make studies on the interaction between skeletal myoblasts and myocardial cells during repair process is of urgency. However, in vivo experiments are under uncertain cues that could intervene in the exploration of skeletal myoblast restoration on myocardial cells, and also could not spatiotemporally control the communication of skeletal muscle cells and myocardial cells.

Recently, numerous studies have demonstrated that microfluidics is a promising platform for spatiotemporal manipulation of mammalian cells and their microenvironment with high microscale resolution.[15,16] Combined with appropriate microstructures and feasible sequential manipulations, microfluidic devices can precisely control fluid perfusion and biological sample localization, as well as keep the organized cells in a tissue-relevant context.[17-19] Microfluidic devices developed for cardiac research have been used to study cardiac electrical activity,[20] cell orientation and mechanical function measurement,[21] drug-induced cardiotoxicity,[22] cell metabolism and communication,[23] as well as cardiac tissueengineering.[24] More recently, we developed a micropillar array-aided tissue interface mimicking microfluidic device for the dynamic study of hypoxia-induced myocardial injury in a microenvironment-controllable manner.[18] Using this microfluidic device, hypoxia-

induced myocardial injury was carried out and the varying apoptotic responses of myocardial cells were temporally monitored and measured. The results show that hypoxia directionally resulted in observable cell shrinkage, cytoskeleton disintegration, mitochondrial membrane potential loss, and caspase-3 activation. All these studies greatly improved the microscale evaluation of myocardial tissue/cell properties, especially the studies on the function of myocardial cells. Nevertheless, the on-chip study of skeletal myoblast transplantation, particularly the spatiotemporally controlled investigation of the interactions between skeletal myoblasts and myocardial cells during myocardial cell repair process, has been less advanced.

Here, we describe a study of skeletal myoblast transplantation for the treatment of hypoxia-induced myocardial injury in a cell transplantation mimicking microfluidic device. Using this device, we first realized simultaneous culture of rat heart myocardium H9c2 cells and rat L6 skeletal myoblasts. Hereafter, a myocardial hypoxia environment was created using carbonyl cyanide p-trifluoromethoxyphenylhydrazone (FCCP). Meanwhile, the dynamics of myocardial cells during hypoxia treatment and after coculture with skeletal myoblasts were

investigated.

Experimental

Design and fabrication of the microfluidic device

The microfluidic device utilized for this study was designed using software AutoCAD (Autodesk, Inc., CA, USA) and fabricated from poly(dimethylsiloxane) (PDMS) using a multilayer soft lithography method.[25,26] For the detailed information, see online Supplementary Information.

Microfluidic cell culture

Rat heart myocardium H9c2 cells and rat L6 skeletal myoblasts (The Chinese Academy of Sciences, Shanghai, China) were used for the cellular experiments. These cells were cultured using high glucose Dulbecco's Modified Eagle Medium (DMEM, Invitrogen, NY, USA) supplemented with 10% FBS, 100 U/mL penicillin, and 100 μg/mL streptomycin in a humidified atmosphere of 5% CO_2 at 37 °C. Prior to seeding cells in the microfluidic device, the device was first sterilized with UV light for 2 h and then coated with collagen-I (200 μg/mL) for another 2 h to promote cell adhesion.[26] After rinsing
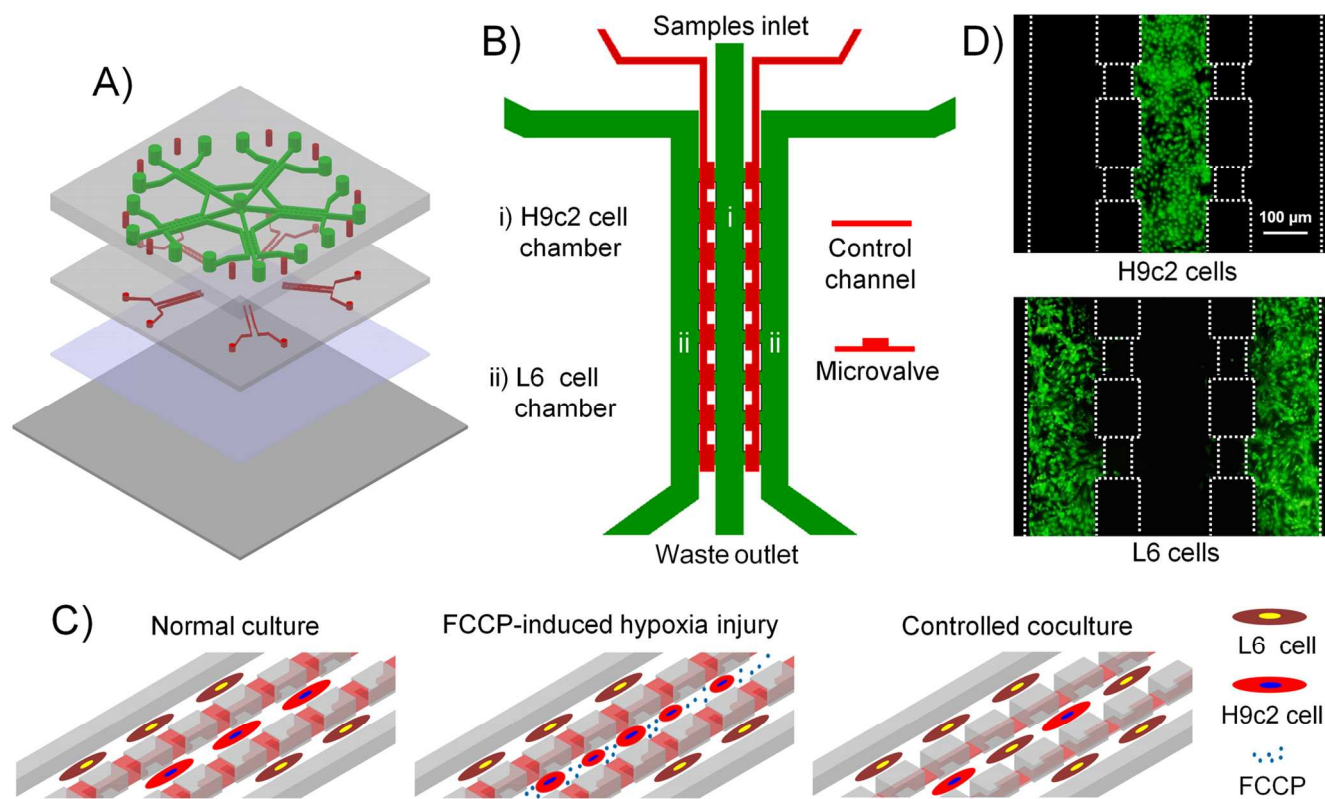
Scheme 1 On-chip monitoring of skeletal myoblast transplantation for the treatment of hypoxia-induced myocardial injury. (A) Composition of the microfluidic device (from top to bottom: fluidic layer, control layer, thin PDMS layer, and glass slide). (B) Schematic representation of a single working unit that contained one H9c2 cell chamber (i) and two L6 cell chambers (ii). Each of the L6 cell chamber was connected with the H9c2 cell chamber via a set of uniformly distributed microchannels, and the communication between the two chambers was regulated by the microvalves embedded in the control matrix. (C) Schematic diagrams showing the on-chip studying procedures (from left to right: normal culture of H9c2 and L6 cells in their respective chambers, hypoxic treatment of H9c2 cells with oxygen consumption blocking reagent FCCP, and the subsequent treatment via coculture with L6 cells. (D) H9c2 cells (top) and L6 cells (bottom) cultured in their respective chambers for 24 h. AO/PI double staining showed that the two cells possessed high viability (green, live cells; and red, dead cells).

thrice with DMEM, H9c2 cells and L6 cells were respectively loaded into their culture chambers by flowing their suspensions (4 μL/min) for 3 min at a cell density of 6.0×10^6 cells/mL. The established microvalve switches prohibited leakage and cross contamination of different cell types in the different chambers. The device was then placed in a humidified atmosphere with 5% CO_2 at 37 °C for 1 h to enable the cells to attach. The supplemented DMEM medium was loaded from the designated inlets into the device to supply culture nutrients to the cells.

Hypoxia-induced myocardial injury and repair via coculture with myoblasts

For the hypoxia treatment of myocardium H9c2 cells, FCCP solution (30 μM in FBS-free DMEM)[18] was continuously introduced into H9c2 cell culture chamber at 1 μL/min for 30 min. Then, FCCP-containing culture medium was replaced with fresh DMEM supplemented with 2% FBS. Meanwhile, the microvalves assembled between the L6 skeletal myoblast and myocardium H9c2 cell culture chambers were opened, and the two types of cells were cocultured for certain duration.
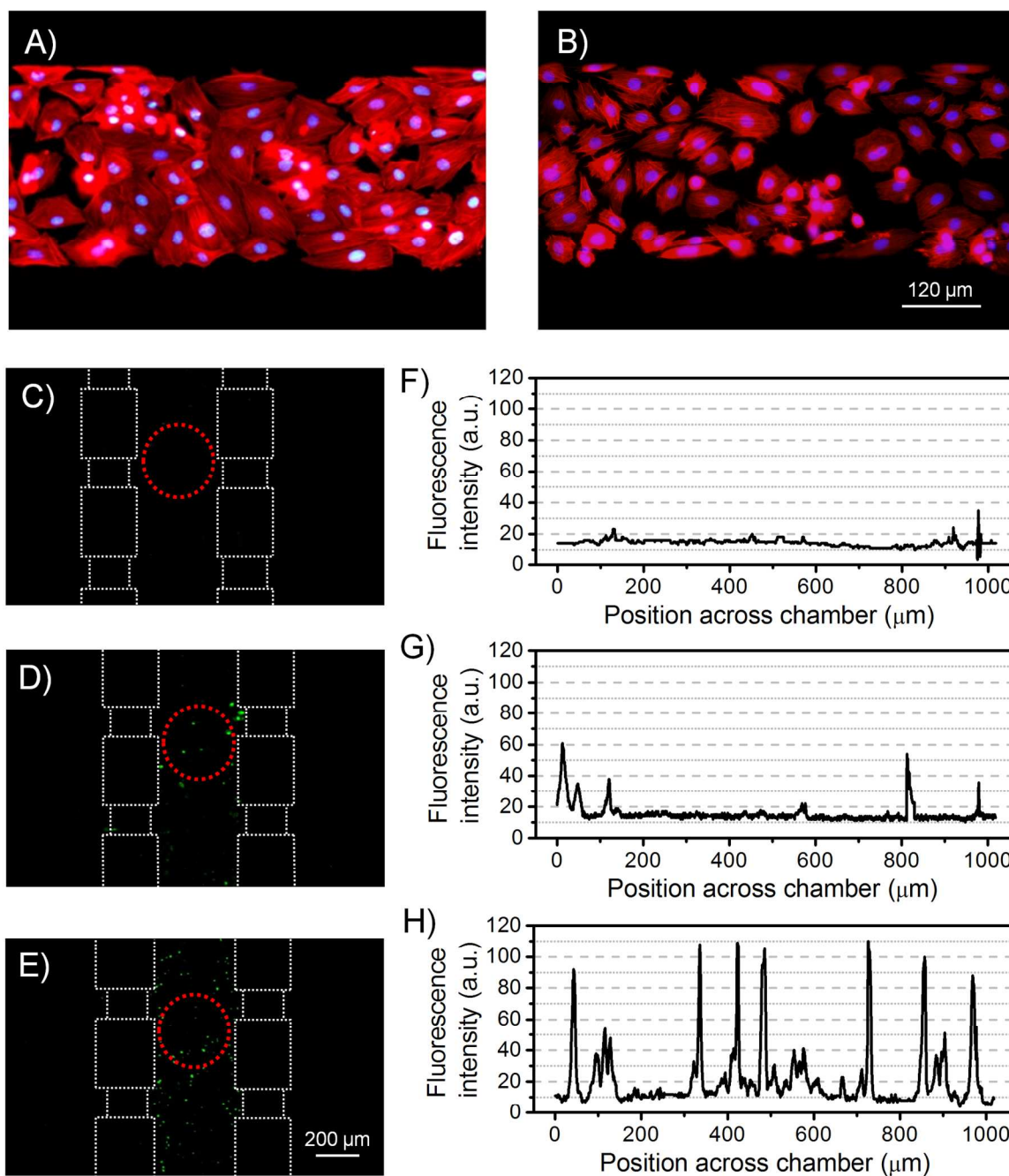
Fig. 1 Evaluation of hypoxia-treated myocardium H9c2 cells. (A) and (B) Fluorescence images of H9c2 cell actin filament (red) and nuclear (blue) under normal culture (A) and after hypoxia treatment with 30 μmol/L FCCP for 0.5 h (B). (C, D and E) Fluorescence images of caspase-3+ cells before hypoxia treatment (C), as well as after 0.5-h (D) and 2-h (E) hypoxia treatment. (F, G and H) Quantitative analysis of fluorescence intensity dynamics of caspase-3+ cells during hypoxia treatment; (F), (G) and (H) correspond to the red dashed circles of (C), (D) and (E), respectively.

Micrographs of cells were captured every 6 h. Each experiment was repeated at least three times in different devices, and in each case, over 180 cells per condition were measured for statistical analysis. Blank controls were run simultaneously during each experiment.

Mitochondrial membrane potential and caspase-3 activity of H9c2 cells

Mitochondrial membrane potential and caspase-3 activity of H9c2 cells were analyzed to evaluate the hypoxic injury and dynamics of myocardial cells. Briefly, the solution of 5,5′,6,6′-tetrachloro-1,1′,3,3′-tetraethyl-benzimidazolylcarbocyanineiodide (JC-1, Biotium; 5 μM) was loaded into the cell culture chamber at a flow rate of 2 μL/min and incubated for 15 min at room temperature before PBS rinsing. The analysis of caspase-3 activation of H9c2 cells was performed using NucView 488 caspase-3 substrate (1 μM; a cell membrane-permeable fluorogenic caspase substrate) with the same procedure as above, except the 30 min incubation time.

Cell staining

Cell viability assessment was performed using the acridine orange (AO)/propidium iodide (PI) double-staining protocol.[26]

Supplementary Information. For clearly distinguishing the coexistence of H9c2 and L6 cells, the two types of cells were respectively stained using CellTracker Green CMFDA and CellTracker Orange CMRA (10 μmol/L in DMEM) before they were loaded into the device for the subsequent studies. To investigate cytoskeleton change before and after treatment with FCCP and coculture with L6 cells, the actin filament of H9c2 cells was also stained.[18] Briefly, the cells were first fixed using 4% paraformaldehyde for 10 min at room temperature after washing thrice with PBS. Then, the cultures were incubated at 37 °C for 20 min with TRITC-phalloidin (100 nM in PBS) following permeabilizing with PBS containing 0.2% Triton X-100 for 30 min. The cell nuclei were stained with Hoechst dye H33258 fluorochrome (0.5 μg/mL) following the same procedures described above.

Microscopy and image analysis

Bright-field and fluorescence images were timely acquired using an inverted microscope (Olympus, CKX41) equipped with a CCD camera (Olympus, DP72) and a mercury lamp (Olympus, U-RFLT50). Software Image-Pro Plus 6.0 (Media Cyternetics) and SPSS12.0 (SPSS Inc.) were used to perform image and statistical data analysis, respectively. The results,
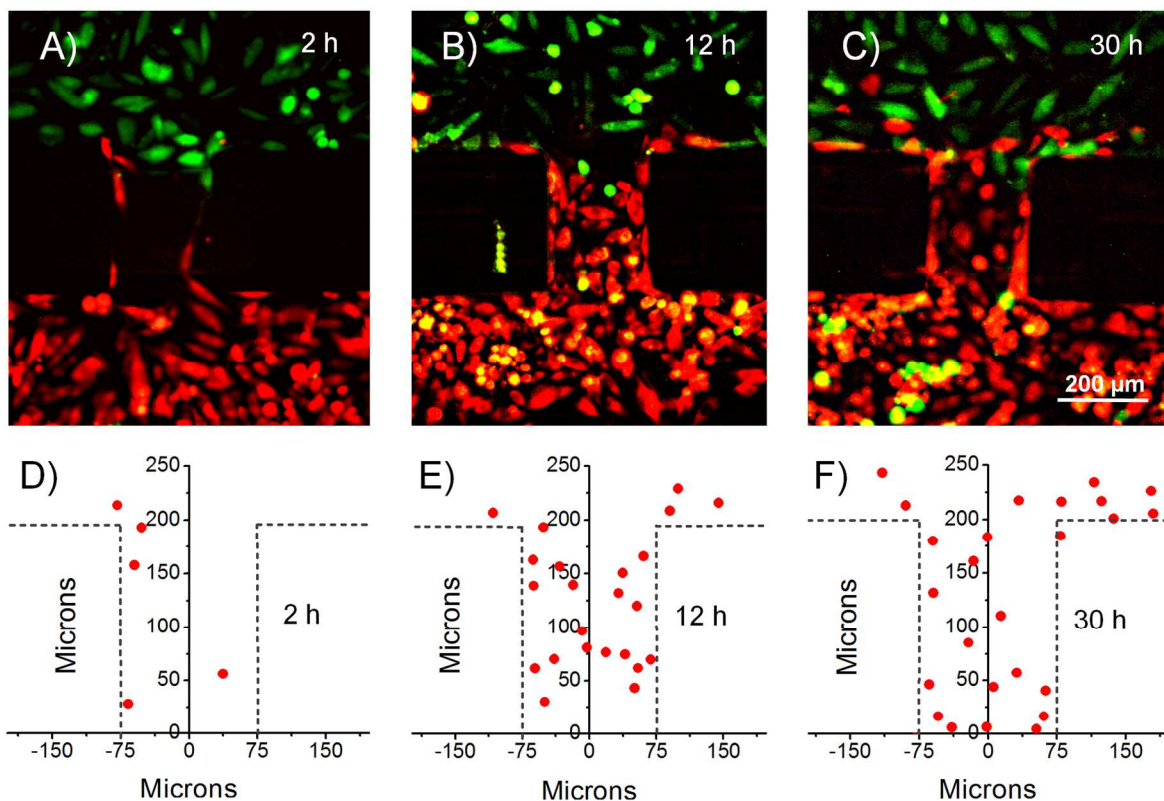
Fig. 2 Migration of L6 cells to H9c2 culture chamber. H9c2 and L6 cells were respectively stained using CellTracker Green and CellTracker Orange. (A, B and C) Time-lapse images of H9c2 and L6 cells after coculture for 2 h (A), 12 h (B) and 30 h (C). (D, E and F) Skeletal myoblasts were represented using red dots and their time-dependent positions were drawn in orthogonal coordinates; (D), (E) and (F) correspond to (A), (B) and (C), respectively. The results showed that L6 cells migrated to the H9c2 culture chamber along the period of coculture. Images were composited by merging two fluorescence channels using Image-Pro Plus 6.0.

The detailed experimental procedures can be found in the

including the error bars in the graphs, were given as the mean ± standard deviation (SD).

Results and discussion

Device design and preparation

The integrated microfluidic device (Scheme 1A) used in the current study was fabricated from PDMS, an optically transparent elastomer widely used in biological microfluidics.[27,28] Generally, the constructed 2.5 cm × 2.5 cm microfluidic device is composed of four layers: the fluidic layer (a microchannel network, μCN), the control layer (a pneumatically actuated microvalve system, PμS), the thin PDMS layer, and a glass slide. The μCN in the fluidic layer contains five units with identical function that could be used for multiple on-chip tests; each unit has a central chamber and two lateral chambers connected by two sets of microchannels (Scheme 1B) where the observation of the coexistence of H9c2 cells and L6 cells was accomplished. The PμS in the control layer was employed to allow manipulation of individual cell culture chamber and spatiotemporally controlled investigation of the interaction between H9c2 and L6 cells. Three inlets and three outlets were used for cell loading, nutrient supply, chamber purging, and waste exclusion. In PμS, two water-filled channels incorporated rectangular cross-shaped microvalves were pressurized to deflect the PDMS membrane upward to

seal off the fluid channel.[26] The thin PDMS layer was used to enable the valves to withstand the high actuation pressure better after irreversibly bonding with the control layer.[29,30] When the microvalves were opened, the medium volume difference between the H9c2 cell and L6 cell reservoirs forced the medium to flow from the L6 cell culture chamber into the H9c2 cell chamber, achieving the communication of two heterogeneous cells, as indicated by fluorescein test (ESI, Figure S1†).

On-chip coculture of myocardium H9c2 cells and skeletal L6 myoblasts

To on-chip mimic in vivo cell transplantation for the treatment of hypoxia-induced myocardial injury, as well as to spatiotemporally controlled study the interactions between skeletal myoblasts and myocardial cells during myocardial cell repair process, we designed and fabricated the microfluidic device aforementioned and myocardium H9c2 cells and skeletal L6 myoblasts (Scheme 1C) were used.[31] H9c2 cells were seeded in the central culture chamber and skeletal L6 myoblasts were seeded in the two lateral chambers assisted by microvalves located under the connected channels. The two type cells exhibited good adhesion and proliferation (Scheme 1D) with high viability (H9c2 cells, 99.5% and L6 cells, 99.1%). In the subsequent study, H9c2 cells and L6 cells were respectively stained using CellTracker Green and CellTracker Orange with the aim of clearly distinguishing the two types of
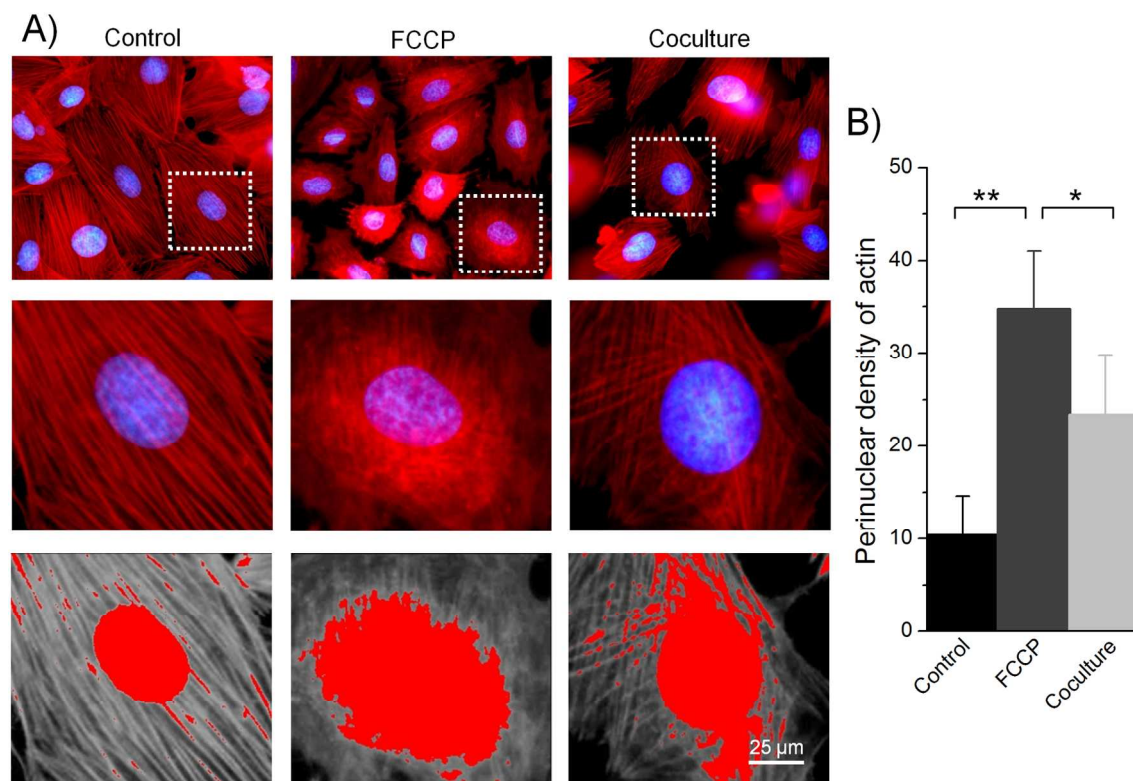
Fig. 3 Analysis of the perinuclear density of H9c2 cell actin. (A) Fluorescence images of actin filament (red) and nuclear (blue) staining (the first and second rows), as well as the morphometric assessment of the perinuclear density of actin (the third row) under various culture conditions [i.e., normal culture condition (Control), hypoxia treatment condition (FCCP), and coculture condition (Coculture)]. The second row is the enlarged images of actin filament and nuclear staining, which corresponds to the white dashed rectangles in the first row. (B) Quantitative analysis of the perinuclear density of H9c2 cell actin after culture under various conditions. Data are given as means ± SD, collected from three independent experiments with at least 180 cells counted. *$P < 0.05$; **$P < 0.005$.

Hypoxia-induced myocardial injury

Myocardial ischemia has been demonstrated to always result in myocardial hypoxia, especially in myocardial infarction.[32] In the current study, we used a chemical hypoxia model in vitro assisted by oxygen consumption blocking reagent FCCP that can reproduce a hypoxic condition similar to the in vivo myocardial ischemia injury.[18,33] FCCP can uncouple the mitochondrial respiratory chain, so oxygen could not involve in the respiratory chain; the oxidative phosphorylation is inhibited and the energy production depends on glycolysis.[33] Initially, the myocardial cells were routinely cultivated in the central chamber for 12 h. Then, the medium was replaced by FCCP-containing medium (without FBS) to create a less nourishing condition that closely simulates a serious myocardial

observable cell response from the imaging results (Fig. 1A and B) was cell shrinkage, which was characterized by a size decreasing gradient, and further, became more serious along with hypoxia time extension (ESI, Figure S2†). The cell morphological change implied that sustained hypoxia could induce aggressive injury to myocardial cells. The injured cells became spatially independent, and were of no connection with each other; moreover, the long actin bundles were damaged and disassembled.

Caspases, a family of cysteine proteases, play essential roles in cell apoptosis and can trigger the apoptotic process of cells when activated.[34] In the current study, the activation signal of caspase-3 during hypoxia treatment was monitored using NucView 488 caspase-3 substrate.[35] The substrate consists of a fluorogenic DNA dye and a DEVD substrate moiety specific for caspase-3, which are both nonfluorescent and nonfunctional
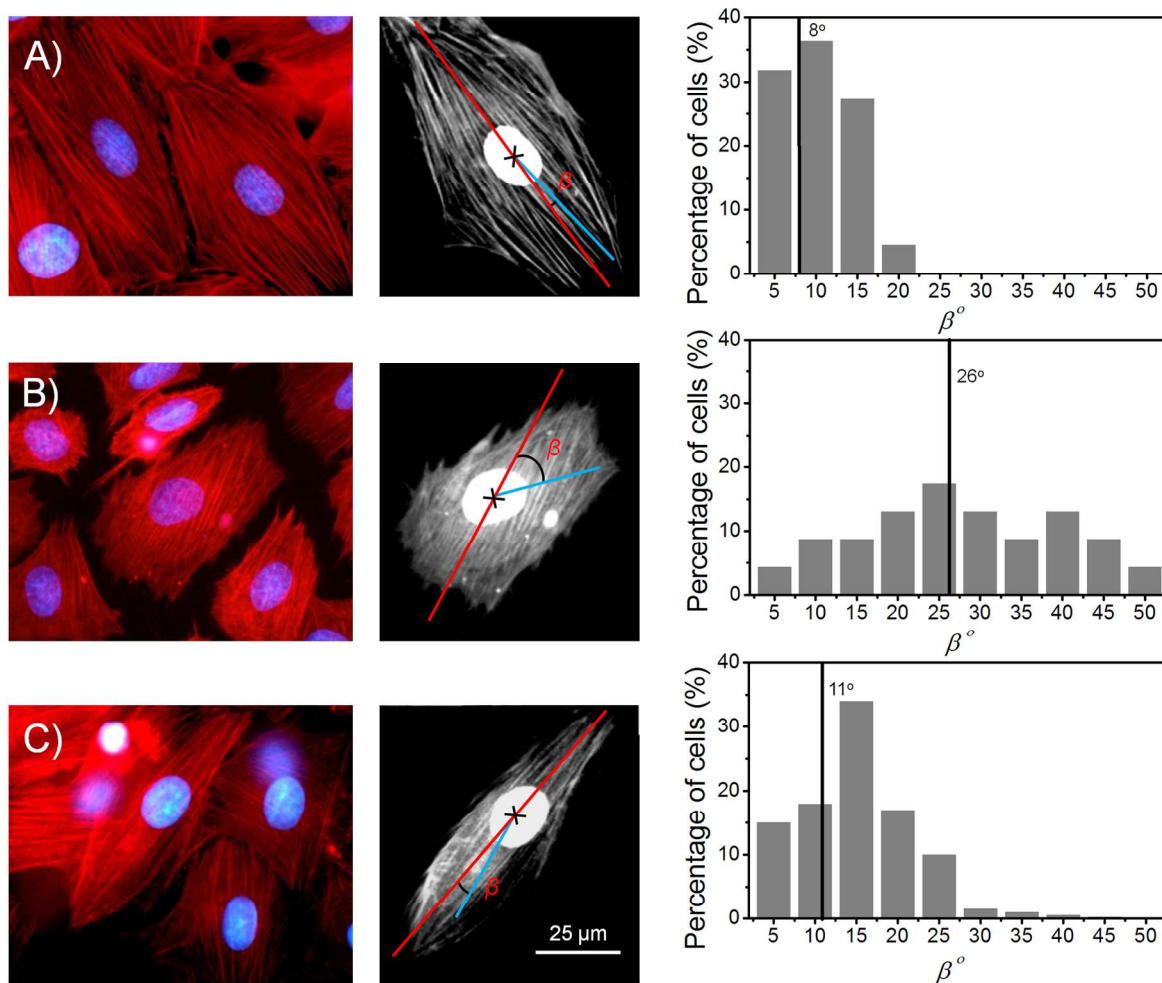
Fig. 4 Assessment of the position relationship of the actin filament arrangement and the nucleus localization at single-cell resolution. 'β' (°) is an acute angle between the long axes defined by the nucleus center (blue line) and the center of the cytoplasmic actin filament area (red line). (A) Morphological image of the actin filament and nucleus under normal culture condition, with its distribution of β. (B) Morphological image of the actin filament and nucleus after hypoxia treatment, with its distribution of β. (C) Morphological image of the actin filament and nucleus after coculture with L6 cells, with its distribution of β. The central point of the black cross is the center of the nucleus. The average angle is indicated in black line. Data were collected from three independent experiments with at least 60 cells counted.

ischemia/hypoxia similar to myocardial infarction.[18] The first

as a DNA dye. After cleavage by caspase-3, a high-affinity

DNA dye was released and stained the nucleus bright green.[18] Analysis of caspase-3 positive cells (caspase-3+ cells) during on-chip hypoxia treatment showed that the percentage of caspase-3+ cells increased with hypoxia time extension (Fig. 1C-H), which indicated that long-time hypoxia treatment could induce more H9c2 cell apoptosis. Comprehensive analysis of the results as well as those reported by us,[18] 30-min hypoxia treatment was used in the next study because moderate injury to H9c2 cells was observed after this time treatment.

Myocardium H9c2 cell repair via coculture with L6 myoblasts

To mimic the in vivo cell transplantation, the interactions between L6 cells and hypoxia-injured H9c2 cells were studied in the microfluidic device. The microvalves assembled between the L6 skeletal myoblast and myocardium H9c2 cell culture chambers were slightly opened to allow either indirect communication through paracrine, or direct communication through cell-to-cell interactions. Cell movement was timely tracked at single-cell resolution to monitor cell migration path. The imaging results (Fig. 2A-C) showed that L6 cells gradually migrated toward the central chamber and formed homogeneous and heterogeneous cell contacts. For a more intuitive understanding of the myoblast migration status, myoblasts migration distance was quantified and drawn in an orthogonal

These results demonstrated that this microfluidic device could perform controllable coculture of two heterogeneous cells, and could be also convenient for monitoring the interactions between H9c2 cells and L6 cells. Analysis of cytoskeletal networks (Fig. 3) of H9c2 cells by TRITC-phalloidin staining actin (one of the primary structural proteins of cardiac muscle) showed that the perinuclear actin filaments were regularly arranged and the perinuclear actin density[36,37] (for the calculation, see the Supplementary Information) was uniformly distributed (Fig. 3, Control) under normal culture condition; after FCCP treatment, the perinuclear actin filaments were vague with irregular arrangement and the perinuclear actin density become stronger with concentrated fluorescence (Fig. 3, FCCP). However, after coculture with L6 cells, the perinuclear actin filament arrangement and the perinuclear actin density presented recovery phenomena (Fig. 3, Coculture). Further analysis of the relationship of cell actin filament arrangement and nucleus localization using a new factor 'β (^{o})' (an acute angle between the long axes defined by the nucleus center and the center of the cytoplasmic actin filament area)[37] showed that the angle β of H9c2 cells under normal culture condition was no more than 25°, with an average of 8° (Fig. 4A). After hypoxia treatment, the angle β was widely distributed with an average of 26° and the maximum angle was even greater than
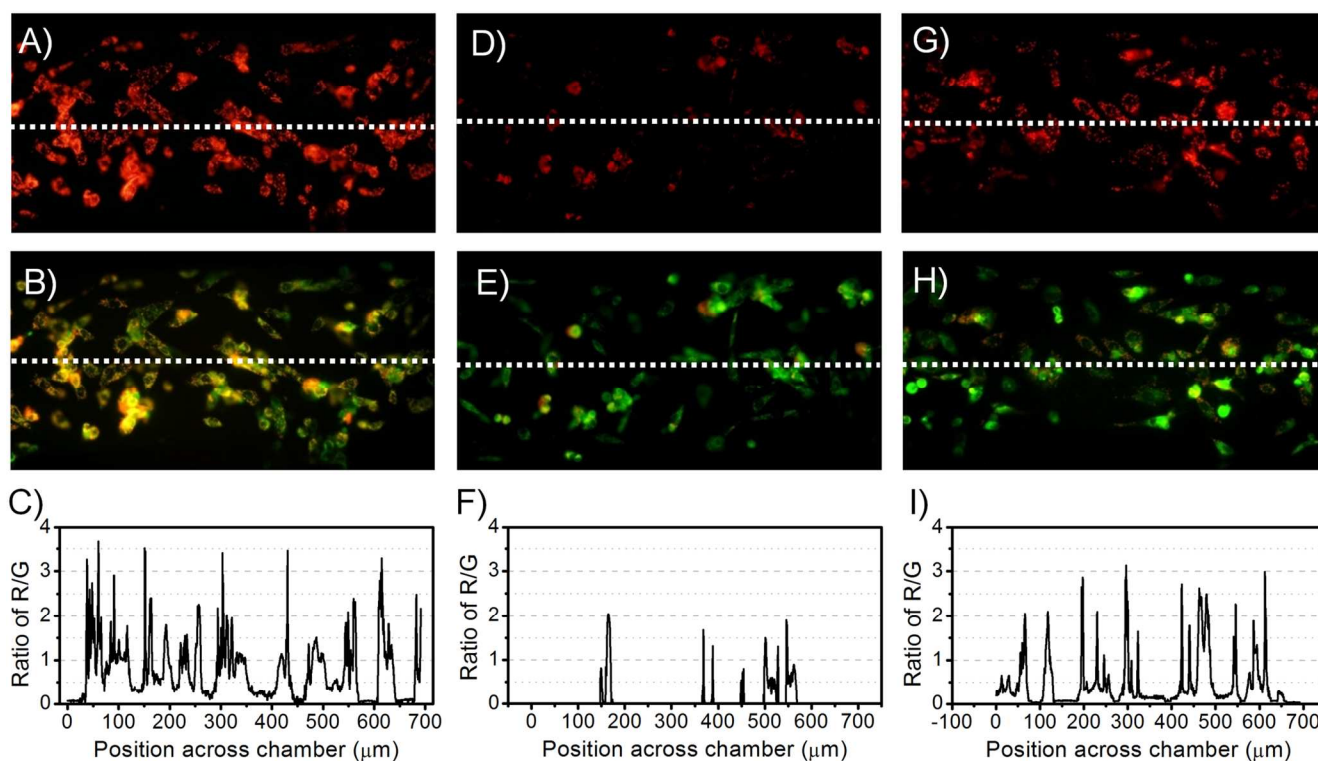
Fig. 5 Quantitative analysis of the mitochondrial membrane potential of H9c2 cells before (A, B and C) and after (D, E and F) 30-min hypoxia treatment, as well as after coculture with L6 cells (G, H and I). (A, D and G) Fluorescence images of JC-1 aggregates in mitochondria before (A) and after (D) 30-min hypoxia treatment, as well as after coculture with L6 cells (G). (B, E and H) Fluorescence images of JC-1 monomers in cytoplasm before (B) and after (E) 30-min hypoxia treatment, as well as after coculture with L6 cells (H). (C, F and I) Ratio of JC-1 aggregates to its monomers before (C) and after (F) 30-min hypoxia treatment, as well as after coculture with L6 cells (I), corresponding to the dotted lines in parts (A) and (B), (D) and (E), as well as (G) and (H), respectively.

coordinate corresponding to the coculture region (Fig. 2D-F).   50° (Fig. 4B). After coculture with L6 skeletal myoblasts, H9c2

cells showed an average of 11° (Fig. 4C). All the results indicated the repair effect of L6 cells on hypoxia-injured H9c2 cells.

To further confirm the repair effect of L6 cells on hypoxia-injured H9c2 cells, the mitochondria membrane potential of H9c2 cells was also monitored (Fig. 5) by using a common cationic dye JC-1. Generally, JC-1 exists in two forms, namely, aggregate and monomer, which can detect the mitochondrial depolarization and membrane potential alteration appeared in the early stage of apoptosis.[38,39] After cellular uptake, JC-1 aggregates in the healthy mitochondria with high membrane potential and emits red fluorescence at 590 nm. On the contrary, JC-1 is monomeric in the membrane-damaged mitochondria with low membrane potential, sequentially leaking into the cytoplasm. The monomer emits green fluorescence at 527 nm and its variability can indirectly show the dynamics of membrane potential.[38,39] For a more accurate assessment, the fluorescence ratio between the two types of JC-1 forms, as a substitute to the simple value of fluorescence intensity, was used to reflect the quantitative change in the membrane potential.[39] The result showed that compared with the normal culture (Fig. 5A-C), the ratio of JC-1 two forms significantly decreased after hypoxia treatment (Fig. 5D-F). While, the ratio increased after cocultured with L6 skeletal myoblasts (Fig. 5G-I). All the results provided supportive evidence that L6 myoblasts could repair hypoxia-induced H9c2 cell injury.

Several possible mechanisms underlying the therapeutic outcome of myocardial repair exerted by skeletal myoblasts have been proposed that skeletal myoblasts may 1) fuse with host cardiomyocytes by partial cell fusion through direct cell-to-cell connection;[40,41] 2) influence the neighboring cardiac tissue by paracrine signaling with release of cytokines and growth factors.[42] However, these probable repair mechanisms by which skeletal myoblasts improve myocardial function are not fully understood and remain largely speculative because limited number of fusion events detected fails to support a substantial improvement of cardiac function.[43] To explore the probable repair mechanism, in the final part of this study, we comparatively investigated two possible factors, one is heterogeneous interaction by direct cell contact, and the other is through paracrine, namely, L6 cells may secrete cytokines into culture medium that may play an essential role in repairing myocardial hypoxia injury. Conditional culture medium from L6 cell culture was used to substitute paracrine and normal culture medium was used as control. The two kinds of cell culture media were respectively used to culture myocardium H9c2 cells. To monitor H9c2 cell change during this test, cell images were taken every 6 h (ESI, Fig. S3 and S4†), which indicate that no obvious change was found in cell morphology and cell viability, whether cultured with normal culture medium, or with conditional culture medium. Cell roundness was considered as an important factor, which can indicate cell viability as well as cell morphology changes. Therefore, cell roundness of H9c2 cells under different conditions were comparatively analyzed in the current study (ESI, Fig. S5†).

The result showed that the introduction of conditional cell culture medium or normal cell culture medium didn't significantly change it after culture for 36 h. However, after coculture with L6 cells, H9c2 cells extended and cell roundness increased with time extension. Further analysis of cell area also showed the similar results (ESI, Fig. S6†). All the results to some extent indicated that the repair of hypoxia-injured myocardium H9c2 by skeletal myoblast L6 cells was mainly through direct heterogeneous cell-to-cell interaction, similar to the study reported previously.[40,41]

Conclusions

In this study, an on-chip assay of skeletal myoblast transplantation for the treatment of hypoxia-induced myocardial injury was carried out in a cell transplantation mimicking microfluidic device. The oxygen consumption blocking reagent FCCP was used to create a hypoxia environment for myocardial injury. Skeletal L6 myoblasts and H9c2 cardiomyoctes were simultaneously cultured in their respective chamber assembled in a single device and their communication was temporally controlled by the switches of microvalves assembled between L6 and H9c2 cell culture chambers. Quantitative analysis of the morphological and pathophysiological dynamics of H9c2 cells showed that after coculture with L6 cells, the cell area of hypoxia-injuried cardiomyoctes increased, perinuclear density of actin augmented, and membrane potential of the mitochondria reversed. All the results implied that L6 skeletal myoblasts could repair the hypoxia-induced cardiomyocte injury. Further investigation by using the conditional medium of L6 skeletal myoblasts demonstrated that skeletal myoblasts morphologically repaired hypoxia-injured myocardium H9c2 cells mainly through direct cell-to-cell interactions.

Acknowledgements

Notes and references

[a] College of Science, Northwest A&F University, Yangling, Shaanxi, 712100, China. Tel: +86-298-708-2520; E-mail: jywang@nwsuaf.edu.cn

[b] College of Veterinary Medicine, Northwest A&F University, Yangling, Shaanxi, 712100, China

† Electronic Supplementary Information (ESI) available: materials and reagents, cell culture, cellular viability assay, design and fabrication of the microfluidic device, on-chip fluidic control test, measurement of perinuclear density of actin, comparison of the effects of conditional culture medium of skeletal myoblast and normal culture medium on myocardial injury healing. See DOI: 10.1039/b000000x/

‡ The two authors contributed equally to this work.

1   B. Cannon, *Nature*, 2013, **493**, s2-s3.

2   A. A. Kocher, M. D. Schuster, M. J. Szabolcs, S. Takuma, D. Burkhoff, J. Wang, S. Homma, N. M. Edwards and S. Itescu, *Nat. Med.*, 2001, **7**, 430-436.

3   P. Menasché, A. A. Hagège, M. Scorsin, B. Pouzet, M. Desnos, D. Duboc, K. Schwartz, J.-T. Vilquin and J.-P. Marolleau, *Lancet*, 2001, **357**, 279-280.

4   H. Kamihata, H. Matsubara, T. Nishiue, S. Fujiyama, Y. Tsutsumi, R. Ozono, H. Masaki, Y. Mori, O. Iba, E. Tateishi, A. Kosaki, S. Shintani, T. Murohara, T. Imaizumi and T. Iwasaka, *Circulation*, 2001, **104**, 1046-1052.

5   M. G. Klug, M. H. Soonpaa, G. Y. Koh and L. J. Field, *J. Clin. Invest.*, 1996, **98**, 216-224.

6   D. Orlic, J. Kajstura, S. Chimenti, F. Limana, I. Jakoniuk, F. Quaini, B. Nadal-Ginard, D. M. Bodine, A. Leri and P. Anversa, *Proc. Natl. Acad. Sci. U. S. A.*, 2001, **98**, 10344-10349.

7   G. Y. Koh, M. H. Soonpaa, M. G. Klug, H. P. Pride, B. J. Cooper, D. P. Zipes and L. J. Field, *J. Clin. Invest.*, 1995, **96**, 2034-2042.

8   M. H. Soonpaa, G. Y. Koh, M. G. Klug and L. J. Field, *Science*, 1994, **264**, 98-101.

9   K. A. Hutcheson, B. Z. Atkins, M. T. Hueman, M. B. Hopkins, D. D. Glower and D. A. Taylor, *Cell Transplant.*, 2000, **9**, 359-368.

10 M. Jain, H. DerSimonian, D. A. Brenner, S. Ngoy, P. Teller, A. S. B. Edge, A. Zawadzka, K. Wetzel, D. B. Sawyer, W. S. Colucci, C. S. Apstein and R. Liao, *Circulation*, 2001, **103**, 1920-1927.

11 S. Tomita, R.-K. Li, R. D. Weisel, D. A. G. Mickle, E.-J. Kim, T. Sakai and Z.-Q. Jia, *Circulation*, 1999, **100**, II-247-II-256.

12 P. Menasché, *J. Mol. Cell. Cardiol.*, 2008, **45**, 545-553.

13 F. D. Pagani, H. DerSimonian, A. Zawadzka, K. Wetzel, A. S. B. Edge, D. B. Jacoby, J. H. Dinsmore, S. Wright, T. H. Aretz, H. J. Eisen and K. D. Aaronson, *J. Am. Coll. Cardiol.*, 2003, **41**, 879-888.

14 M. Philippe, A. A. Hagège, J.-T. Vilquin, M. Desnos, E. Abergel, B. Pouzet, A. Bel, S. Sarateanu, M. Scorsin, K. Schwartz, P. Bruneval, M. Benbunan, J.-P. Marolleau and D. Duboc, *J. Am. Coll. Cardiol.*, 2003, **41**, 1078-1083.

15 G. M. Whitesides, *Nature*, 2006, **442**, 368-373.

16 A. Khademhosseini, R. Langer, J. Borenstein and J. P. Vacanti, *Proc. Natl. Acad. Sci. U. S. A.*, 2006, **103**, 2480-2487.

17 D. Huh, B. D. Matthews, A. Mammoto, M. Montoya-Zavala, H. Y. Hsin and D. E. Ingber, *Science*, 2010, **328**, 1662-1668.

18 L. Ren, W. Liu, Y. Wang, J.-C. Wang, Q. Tu, J. Xu, R. Liu, S.-F. Shen and J. Wang, *Anal. Chem.*, 2013, **85**, 235-244.

19 K. R. Stevens, M. D. Ungrin, R. E. Schwartz, S. Ng, B. Carvalho, K. S. Christine, R. R. Chaturvedi, C. Y. Li, P. W. Zandstra, C. S. Chen and S. N. Bhatia, *Nat. Commun.*, 2013, **4**, No. 1847.

20 G. Gaudesius, M. Miragoli, S. P. Thomas and S. Rohr, *Circ. Res.*, 2003, **93**, 421-428.

21 Y. Zhao, C. C. Lim, D. B. Sawyer, R. Liao and X. Zhang, *Cell Motil. Cytoskeleton*, 2007, **64**, 718-725.

22 M. J. Kim, S. C. Lee, S. Pal, E. Han and J. M. Song, *Lab Chip*, 2011, **11**, 104-114.

23 W. Cheng, N. Klauke, G. Smith and J. M. Cooper, *Electrophoresis*, 2010, **31**, 1405-1413.

24 A. Grosberg, P. W. Alford, M. L. McCain and K. K. Parker, *Lab Chip*, 2011, **11**, 4165-4173.

25 L. Li, L. Ren, W. Liu, J.-C. Wang, Y. Wang, Q. Tu, J. Xu, R. Liu, Y. Zhang, M.-S. Yuan, T. Li and J. Wang, *Anal. Chem.*, 2012, **84**, 6444-6453.

26 W. Liu, L. Li, X. Wang, L. Ren, X. Wang, J. Wang, Q. Tu, X. Huang and J. Wang, *Lab Chip*, 2010, **10**, 1717-1724.

27 P. Sun, Y. Liu, J. Sha, Z. Zhang, Q. Tu, P. Chen and J. Wang, *Biosens. Bioelectron.*, 2011, **26**, 1993-1999.

28 W. Liu, L. Li, J.-C. Wang, Q. Tu, L. Ren, Y. Wang and J. Wang, *Lab Chip*, 2012, **12**, 1702-1709.

29 M. A. Unger, H.-P. Chou, T. Thorsen, A. Scherer and S. R. Quake, *Science*, 2000, **288**, 113-116.

30 T. Thorsen, S. J. Maerkl and S. R. Quake, *Science*, 2002, **298**, 580-584.

31 S. J. Watkins, G. M. Borthwick and H. M. Arthur, *In Vitro Cell Dev. Biol. Anim.*, 2011, **47**, 125-131.

32 H. Shimokawa and S. Yasuda, *J. Cardiol.*, 2008, **52**, 67-78.

33 X. Li, L. Zhao, Z. Chen, Y. Lin, P. Yu and L. Mao, *Anal. Chem.*, 2012, **84**, 5285-5291.

34 J. Li and J. Yuan, *Oncogene*, 2008, **27**, 6194-6206.

35 G. Monaco, E. Decrock, H. Akl, R. Ponsaerts, T. Vervliet, T. Luyten, M. De Maeyer, L. Missiaen, C. W. Distelhorst, H. De Smedt, J. B. Parys, L. Leybaert and G. Bultynck, *Cell Death Differ.*, 2012, **19**, 295-309.

36 D. J. Webb, K. Donais, L. A. Whitmore, S. M. Thomas, C. E. Turner, J. T. Parsons and A. F. Horwitz, *Nat Cell Biol*, 2004, **6**, 154-161.

37 I. Dupin, Y. Sakamoto and S. Etienne-Manneville, *J. Cell Sci.*, 2010, **124**, 865-872.

38 J.-S. Wu, T.-N. Lin and K. K. Wu, *J. Cell Physiol.*, 2009, **220**, 58-71.

39 G. Dispersyn, R. Nuydens, R. Connors, M. Borgers and H. Geerts, *Biophysica Acta*, 1999, **1428**, 357-371.

40 L. Formigli, F. Francini, A. Tani, R. Squecco, D. Nosi, L. Polidori, S. Nistri, L. Chiappini, V. Cesati, A. Pacini, A. M. Perna, G. E. Orlandini, S. Zecchi Orlandini and D. Bani, *Am. J. Physiol. Cell Physiol.*, 2005, **288**, C795-C804.

41 H. Reinecke, E. Minami, V. Poppa and C. E. Murry, *Circ. Res.*, 2004, **94**, e56-e60.

42 H. Ebelt, M. Jungblut, Y. Zhang, T. Kubin, S. Kostin, A. Technau, S. Oustanina, S. Niebrugge, J. Lehmann, K. Werdan and T. Braun, *Stem cells*, 2007, **25**, 236-244.

43 J. J. Gavira, G. Abizanda, M. Perez-Ilzarbe, D. Martinez-Caro, E. Nasarre, A. Perez-Ruiz and F. Prosper, *Eur. Heart J.*, 2008, **10** (Supplements K), K11-K15.

Graphical abstract
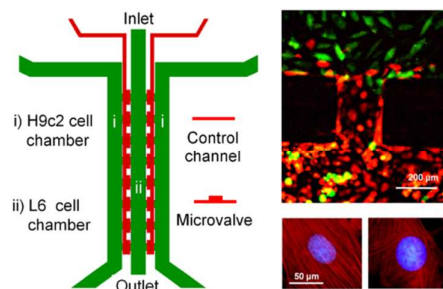
We present a microfluidic method for the assay of skeletal myoblast transplantation for the treatment of hypoxia-induced myocardial injury.